

A model for gluon production in heavy-ion collisions at the LHC with rcBK unintegrated gluon densities

Javier L. Albacete^{a*}, Adrian Dumitru^{b†}

^a*Institut de Physique Théorique - CEA/Saclay, 91191 Gif-sur-Yvette cedex, France.*

^b*Department of Natural Sciences, Baruch College, CUNY, 17 Lexington Avenue, New York, NY 10010, USA
RIKEN BNL Research Center, Brookhaven National Laboratory, Upton, NY 11973, USA*

October 31, 2011

Abstract

This note is a physics manual for a recent numerical implementation of k_t -factorization with running-coupling BK unintegrated gluon distributions. We also compile some results for Pb+Pb collisions at $\sqrt{s} = 2.75$ TeV, such as predictions for the centrality dependence of the charged particle multiplicity, transverse energy, and eccentricity. The model can further be used to obtain initial conditions for hydrodynamic simulations of A+A collisions at the LHC.

1 Introduction

In this note we describe some of the physics underlying a recent numerical implementation of k_t -factorization with running-coupling BK unintegrated gluon distributions for heavy-ion (and pp, pA) collisions at the RHIC and LHC colliders. Its main purpose is to describe the framework as well as some of the main assumptions and model parameters which could be tested by comparing to upcoming data from heavy-ion collisions at the LHC.

Further, the model may be useful for obtaining initial conditions for hydrodynamic simulations of A+A collisions. Below, we also summarize a few key results. The C++ code is available for download at

http://physics.baruch.cuny.edu/node/people/adumitru/res_cgc.

In this “manual” we do not provide an overview of the theory or applications of the Color Glass Condensate.

2 The running coupling BK equation

The Color Glass Condensate is equipped with a set of renormalization group equations, the B-JIMWLK equations, which describe the quantum evolution of hadron structure towards small- x

*e-mail: javier.lopez-albacete@cea.fr

†Adrian.Dumitru@baruch.cuny.edu

(see e.g. [1, 2, 3] and references therein). The B-JIMWLK equations are equivalent to an infinite set of coupled non-linear integro-differential evolution equations for the expectation values of the different correlators of Wilson lines averaged over the target gluon field configurations. In the large- N_c limit the full B-JIMWLK hierarchy reduces to the Balitsky-Kovchegov (BK) [4, 5] equation: a single, closed equation for the the forward scattering amplitude of a $q\bar{q}$ dipole on a dense target

$$\mathcal{N}(\underline{x}, \underline{y}, Y) = 1 - \frac{1}{N_c} \langle U(\underline{x}) U^\dagger(\underline{y}) \rangle_Y \quad (1)$$

where the U 's denote Wilson lines in the fundamental representation, \underline{x} (\underline{y}) is the transverse position of the quark (antiquark) and $\underline{r} = \underline{x} - \underline{y}$ the dipole transverse size. The average over the target gluon field configurations is performed at evolution rapidity $Y = \ln(x_0/x)$, where x_0 is the starting point for the evolution. The BK equation reads:

$$\frac{\partial \mathcal{N}(r, x)}{\partial \ln(x_0/x)} = \int d^2 \underline{r}_1 K(\underline{r}, \underline{r}_1, \underline{r}_2) [\mathcal{N}(r_1, x) + \mathcal{N}(r_2, x) - \mathcal{N}(r, x) - \mathcal{N}(r_1, x) \mathcal{N}(r_2, x)] \quad (2)$$

where K is the evolution kernel and $\underline{r}_2 = \underline{r} - \underline{r}_1$. In Eq. (2) we have implicitly assumed translational invariance over scales of order the nucleon radius, i.e. that the dipole amplitude depends only on the dipole transverse size $r \equiv |\underline{r}|$ but not on the impact parameter $\underline{b} = (\underline{x} + \underline{y})/2$ of the collision¹. A smooth variation of $\mathcal{N}(r, x)$ on larger distance scales can be incorporated via the initial condition at the starting point x_0 of the evolution, see below.

The original BK equation resums small- x gluon emission to all orders at leading-logarithmic (LL) accuracy in $\alpha_s \ln(x_0/x)$, with α_s fixed, and also contains non-linear terms that account for gluon-gluon self-interactions, relevant in a high density scenario. However, such limited dynamical input does not suffice to provide a good description of experimental data. This situation has been considerably improved by the recent determination of running corrections to the LL equations [7, 8, 9]. Such corrections amount to just a modification of the evolution kernel in Eq. (2) with respect to the LL result. Though there are different possibilities of defining the running coupling kernel, it was shown in [10] that the prescription proposed by Balitsky in [8] minimizes the role of additional *conformal* corrections that arise at the same order as the running coupling, making it better suited for phenomenological applications. The corresponding running coupling kernel reads

$$K^{\text{run}}(\mathbf{r}, \mathbf{r}_1, \mathbf{r}_2) = \frac{N_c \alpha_s(r^2)}{2\pi^2} \left[\frac{1}{r_1^2} \left(\frac{\alpha_s(r_1^2)}{\alpha_s(r_2^2)} - 1 \right) + \frac{r^2}{r_1^2 r_2^2} + \frac{1}{r_2^2} \left(\frac{\alpha_s(r_2^2)}{\alpha_s(r_1^2)} - 1 \right) \right] \quad (3)$$

We shall refer to Eq. (2) together with the evolution kernel Eq. (3) as the running coupling BK (rcBK) equation. Running coupling corrections have proven essential for promoting the BK equation to a phenomenological tool. Indeed, the rcBK equation has been employed successfully to describe inclusive structure functions in e+p scattering [11, 12], the energy and rapidity dependence of hadron multiplicities in Au+Au collisions at RHIC [13], as well as single inclusive spectra in p+p and d+Au collisions at RHIC [14]. A detailed discussion on the numerical set up employed to solve the rcBK equation can be found in [10]. The present model differs from earlier predictions published in ref. [13] mainly due to the initial conditions described below.

Eq. (2) needs to be supplemented with initial conditions. We consider two different families of initial conditions labeled by the parameter γ :

$$\mathcal{N}(r, Y=0; R) = 1 - \exp \left[- \frac{(r^2 Q_{s0}^2(R))^\gamma}{4} \ln \left(\frac{1}{\Lambda r} + e \right) \right], \quad (4)$$

¹This is the main reason why we presently refrain from applying the model to compute the energy dependence of the multiplicity in pp collisions; accurate results require this input, see for example [6].

where $\Lambda = 0.241$ GeV. For each of these families there are two free parameters: the value x_0 where the evolution starts, which we fix it to $x_0 = 0.01$ in all cases, and the initial saturation scale $Q_{s0}(R)$ at the transverse coordinate R . It measures the local density of large- x sources at a fixed point in impact parameter space (i.e., in the transverse plane). The case $\gamma = 1$ corresponds to the McLerran-Venugopalan model. For a single nucleon we take the value $Q_{s0}^2 = 0.2$ GeV² for it and we refer to it in the plots below as MV ic. However, global fits to structure functions in electron+proton scattering at small- x based on rcBK dynamics [11, 12] clearly indicate that a value $\gamma > 1$ is preferred by the data. Following the results in [12]², we take the values $Q_{s0}^2 = 0.168$ GeV² (for a single nucleon) and $\gamma = 1.119$. We refer to this other set of initial conditions as MV $\gamma=1.119$. The value of γ determines the steepness of the unintegrated gluon distribution for momenta above the saturation scale $k_t > Q_s$, the MV $\gamma=1.119$ initial conditions yielding a steeper falloff than the MV ones for all the evolution rapidities relevant at RHIC and the LHC (see fig. 1 bottom). The main novelty in this updated version of the manual is the introduction of this new set of initial conditions with $\gamma > 1$.

As explained in more detail below, the geometry of a given A+A collision is determined by the fluctuations in the positions of the nucleons in the transverse plane. Each configuration defines a different local density in the transverse plane of each nucleus. Obviously, the smallest non-zero local density corresponds to the presence of a single nucleon. On the other hand, in A+A collisions rare fluctuations can result in collisions of a large number of nucleons at the same transverse position and, therefore, in a large Q_{s0} . To account for all possible configurations we tabulate the solution of the rcBK equation for different values of the initial local density, i.e., for each value of $Q_{s0}(R)$ in Eq. (4) ranging from $Q_{s0}^2 = 0.2$ (0.168) GeV² for MV (MV $\gamma=1.119$) initial conditions (for a single nucleon) to $n \times Q_{s0}^2$ with $n = 1 \dots 30$. The solutions are then used in the k_t -factorization formula to calculate local gluon production at each point in the collision zone. Finally we perform the average over all the nucleon configurations generated by the Monte Carlo.

To complete our discussion of the initial conditions we explain how we construct $Q_{s0}(\mathbf{R})$. We first generate a configuration of nucleons for each of the colliding nuclei. This consists of a list of random coordinates \mathbf{r}_i , $i = 1 \dots A$, chosen from a Woods-Saxon distribution. Multi-nucleon correlations are neglected except for imposing a short-distance hard core repulsion which enforces a minimal distance ≈ 0.4 fm between any two nucleons. After this step, the longitudinal coordinate of any nucleon is discarded, they are projected onto the transverse plane. Factorizing the fluctuations of the nucleons in a nucleus from possible fluctuations of large- x “hot spots” within a nucleon (not accounted for at present), and finally from semi-hard gluon production appears to be justified by the scale hierarchy

$$\frac{1}{Q_s} \ll R_N \ll R_A, \quad (5)$$

where R_A , R_N are the radii of a nucleus and of a proton, respectively.

For a given configuration, the initial saturation momentum $Q_{s0}(\mathbf{R})$ at the transverse coordinate \mathbf{R} is taken to be

$$Q_{s0}^2(\mathbf{R}) = N(\mathbf{R}) Q_{s0,\text{nucl}}^2, \quad (6)$$

where $Q_{s0,\text{nucl}}^2 = 0.2$ GeV² for our original uGD with MV model initial conditions while $Q_{s0,\text{nucl}}^2 = 0.168$ GeV² for the new uGD with MV $\gamma=1.119$ initial condition, as discussed above. $N(\mathbf{R})$ is the number of nucleons from the given nucleus which “overlap” the point \mathbf{R} :

$$N(\mathbf{R}) = \sum_{i=1}^A \Theta \left(\sqrt{\frac{\sigma_0}{\pi}} - |\mathbf{R} - \mathbf{r}_i| \right). \quad (7)$$

²Different parameter sets are obtained in [12]. The values (Q_{s0}^2, γ) considered here correspond to fit h') in Table 1, which provide a best fit to data $\chi^2/d.o.f = 1.104$.

Some care must be exercised in choosing the transverse area σ_0 of the large- x partons of a nucleon. Q_{s0} corresponds to the density of large- x sources with $x > x_0$ and should therefore be energy independent (recoil of the sources is neglected in the small- x approximation). We therefore take $\sigma_0 \simeq 42$ mb to be given by the inelastic cross-section at $\sqrt{s} = 200$ GeV. However, σ_0 should not be confused with the energy dependent inelastic cross section $\sigma_{\text{in}}(s)$ of a nucleon which grows due to the emission of small- x gluons.

3 k_t -factorization

According to the k_t -factorization formalism [15], the number of gluons produced per unit rapidity at a transverse position \mathbf{R} in A+B collisions is given by

$$\frac{dN^{A+B \rightarrow g}}{dy d^2p_t d^2R} = \frac{1}{\sigma_s} \frac{d\sigma^{A+B \rightarrow g}}{dy d^2p_t d^2R}, \quad (8)$$

where σ_s represents the effective interaction area and $\sigma^{A+B \rightarrow g}$ is the cross section for inclusive gluon production:

$$\frac{d\sigma^{A+B \rightarrow g}}{dy d^2p_t d^2R} = K \frac{2}{C_F} \frac{1}{p_t^2} \int^{p_t} \frac{d^2k_t}{4} \int d^2b \alpha_s(Q) \varphi\left(\frac{|p_t + k_t|}{2}, x_1; b\right) \varphi\left(\frac{|p_t - k_t|}{2}, x_2; R - b\right), \quad (9)$$

with $x_{1(2)} = (p_t/\sqrt{s_{NN}}) \exp(\pm y)$ and $C_F = (N_c^2 - 1)/2N_c$. As noted before, we assume that the local density in each nucleus is homogenous over transverse distances of the order of the nucleon radius R_N . Thus, the b -integral in Eq. (9) yields a geometric factor proportional to the transverse “area” of a nucleon which cancels with a similar factor implicit in σ_s from Eq. (8), modulo subtleties in the definition of σ_s .

The unintegrated gluon distributions (ugd’s) φ entering Eq. (9) are related to the dipole scattering amplitude in the adjoint representation, \mathcal{N}_G , through a Fourier transform (for consistency with the notation used in Eq. (9) we make the impact parameter dependence of the ugd’s explicit):

$$\varphi(k, x, b) = \frac{C_F}{\alpha_s(k) (2\pi)^3} \int d^2\mathbf{r} e^{-i\mathbf{k}\cdot\mathbf{r}} \nabla_{\mathbf{r}}^2 \mathcal{N}_G(r, Y = \ln(x_0/x), b). \quad (10)$$

In turn, \mathcal{N}_G is related to the quark dipole scattering amplitude that solves the rcBK equation, \mathcal{N} , as follows:

$$\mathcal{N}_G(r, x) = 2\mathcal{N}(r, x) - \mathcal{N}^2(r, x). \quad (11)$$

Note that this relation entails that the saturation momentum relevant for gluon scattering is larger than that for quark scattering by about a factor of 2.

Eqs. (10) and (9) were written originally for fixed coupling. In order to be consistent with our treatment of the small- x evolution, we have extended them by allowing the coupling to run with the momentum scale. The argument of the running coupling in Eq. (9) is chosen to be $Q = \max\{|p_t + k_t|/2, |p_t - k_t|/2\}$, while for the definition of the ugd Eq. (10) we take it to be the transverse momentum itself, k . This turns out to be important in order to reproduce the centrality dependence of charged particle multiplicities at RHIC, which are otherwise too flat for small N_{part} . However, the results are not very sensitive to the particular choice of scale because $\varphi \rightarrow 0$ as $k^2 \rightarrow 0$ due to the saturation of $\mathcal{N}(r)$ at large dipole sizes r . In principle, one could improve on this educated ansatz by using the results of [16] where running coupling corrections to inclusive gluon production have been studied. Most importantly, the x -dependence of the dipole scattering amplitude obtained by solving the rcBK equation encodes all the collision energy and rapidity dependence of the gluon production formula Eq. (9).

The normalization factor $K \simeq 2$ introduced in the k_t -factorization formula (9) above is fixed by the charged particle transverse momentum distribution in p+p collisions at 7 TeV, see below. It lumps together higher-order corrections, sea-quark contributions, a nucleon geometry factor, and so on. We apply an additional “gluon multiplication factor” $\kappa_g \simeq 5$ when computing p_\perp -integrated yields (see below) in heavy-ion collisions but not for the transverse energy dE_t/dy or for high- p_t hadron production in p+p from fragmenting hard gluons.

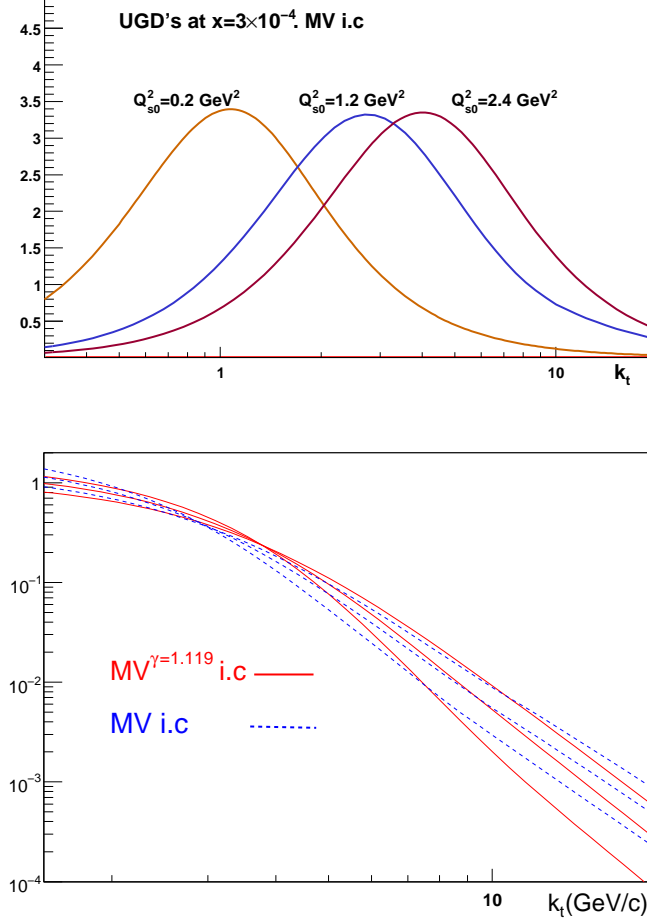


Figure 1: Unintegrated gluon distributions for different values of the initial saturation scale evolved to $x = 3 \cdot 10^{-4}$ (top) for MV i.c (top). UGD's for the two different initial conditions in the single nucleon case: $MV^{\gamma=1.119}$ (solid) and MV (dashed) at rapidities $Y = \ln(x_0/x) = 1.5, 3$ and 6 (bottom).

In fig. 1 (top) we plot the ugd for three different initial MV saturation scales at $x = 3 \cdot 10^{-4}$ versus transverse momentum. The ugd corresponding to a single nucleon peaks at about $k_t \simeq 1 \text{ GeV}$. The ugd's for larger Q_{s0}^2 illustrate the shift predicted for a 6-nucleon and 12-nucleon target, respectively. The bottom plot shows the different k_t slopes for the two initial conditions ($MV^{\gamma=1.119}$ and MV) considered in this work in the single nucleon case.

3.1 Observables

Eq. (9) is the starting point for all observables shown below. In particular, the charged particle multiplicity and the transverse energy can be obtained by integrating over the transverse plane

and p_t ,

$$\frac{dN_{\text{ch}}}{dy} = \frac{2}{3}\kappa_g \int d^2R \int d^2p_t \frac{dN^{A+B \rightarrow g}}{dy d^2p_t d^2R} \quad (12)$$

$$\frac{dN_{\text{ch}}}{d^2p_t dy} = \int d^2R \int \frac{dz}{z^2} D_h(z = \frac{p_t}{k_t}) \frac{dN^{A+B \rightarrow g}}{dy d^2k_t d^2R} \quad (13)$$

$$\frac{dE_t}{dy} = \int d^2R \int d^2p_t p_t \frac{dN^{A+B \rightarrow g}}{dy d^2p_t d^2R} . \quad (14)$$

Note that a low- p_t cutoff is not required since the integration over k_t in (9) extends only up to p_t . The saturation of the gluon distribution functions guarantees that the dominant scale in the transverse momentum integrations is the saturation momentum. For the single-inclusive hadron p_t distributions (13) we use the KKP gluon \rightarrow charged hadron LO fragmentation function [17] with the scale $Q^2 = k_t^2$; the integral over the hadron momentum fraction is restricted to $z \geq 0.05$ to avoid a violation of the momentum sum rule. The “gluon multiplication factor” is fixed to $\kappa_g = 5$ (energy and centrality independent) in order to reproduce the measured charged hadron multiplicity in heavy-ion collisions at RHIC and LHC energies, see below. The upper limit in the integrals over the gluon transverse momentum in dN_{ch}/dy and dE_t/dy has been taken as $p_t^{\text{max}} = 12$ GeV; if the integrals are extended further then a slight adjustment of the normalization factors κ_g and K may be required.

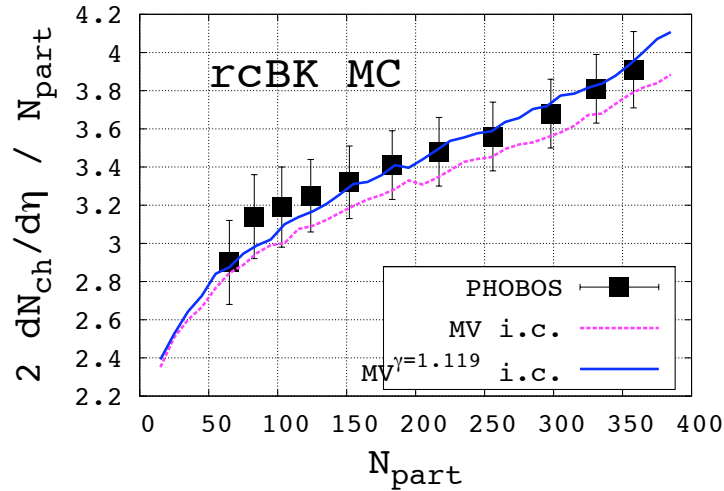


Figure 2: Centrality dependence of the charged particle multiplicity at midrapidity for Au+Au collisions at $\sqrt{s} = 200$ GeV. PHOBOS data: ref. [18].

In order to compare our results for initial gluon production to the final state distributions of detected particles one has to translate the rapidity distributions into pseudo-rapidity distributions through the $y \rightarrow \eta$ Jacobian,

$$\frac{dN_{\text{ch}}}{d\eta} = \frac{\cosh \eta}{\sqrt{\cosh^2 \eta + m^2/P^2}} \frac{dN_{\text{ch}}}{dy} \quad (15)$$

$$\frac{dE_t}{d\eta} = \frac{\cosh \eta}{\sqrt{\cosh^2 \eta + m^2/P^2}} \frac{dE_t}{dy} , \quad (16)$$

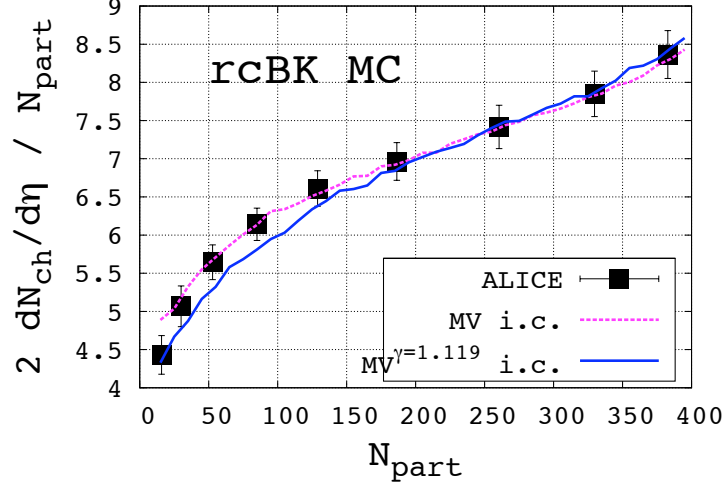


Figure 3: Centrality dependence of the charged particle multiplicity at midrapidity for Pb+Pb collisions at $\sqrt{s} = 2.76$ TeV. Alice data from ref. [19].

with $y = \frac{1}{2} \ln(\sqrt{\cosh^2 \eta + m^2/P^2} + \sinh \eta) / (\sqrt{\cosh^2 \eta + m^2/P^2} - \sinh \eta)$. We assume that in this Jacobian $m = 350$ MeV and $P = 0.13 \text{ GeV} + 0.32 \text{ GeV} \sqrt{s/1 \text{ TeV}}^{0.115}$. Note that such transformation is not needed (it is trivial) if one is interested in initial (massless) gluon production to initialize a hydrodynamic simulation.

4 Results

In this section we present some results obtained with the new $\text{MV}^{\gamma=1.119}$ uGD and compare them to the original uGD obtained by rcBK evolution with MV model initial conditions.

In Fig. 2 we show the centrality dependence of $dN/d\eta$ at full RHIC energy. This energy probes mainly the initial condition for small- x evolution. Both sets perform reasonably well and we do not find it possible to distinguish.

Fig. 3 shows the centrality dependence of $dN/d\eta$ at $\eta = 0$ for Pb+Pb collisions at $\sqrt{s} = 2.76$ TeV ³. Once again both uGD sets agree with the data to within a few percent. It is worth noting that our present results for the multiplicity in central collisions are higher than the one predicted in ref. [13], which also relied on the rcBK equation plus k_t -factorization. The main difference between these two works relates to the treatment of the geometry of the collision: while in [13] the full nucleus was characterized by a single average saturation scale and then evolved to higher energies, the Monte Carlo approach presented here allows for different local densities at every point in the transverse plane, each of them evolved locally to higher energies. The average over different configurations is performed after the evolution, and not before, as implicitly done in [13]. Thus we interpret these two different results as an indication that the average over nuclear geometry does not commute with the evolution.

In Fig. 4 we show the transverse momentum distribution of charged particles for p+p collisions at $\sqrt{s} = 7$ TeV. We recall that presently we assume uniform and homogeneous, “disc-like” nucleons. However, we do not attempt to compute the inelastic proton-proton cross section and high- p_t hadron spectra may not be very sensitive to the proton impact parameter profile.

³The Alice papers summarize other recent predictions for $dN_{\text{ch}}/d\eta$ for Pb+Pb collisions.

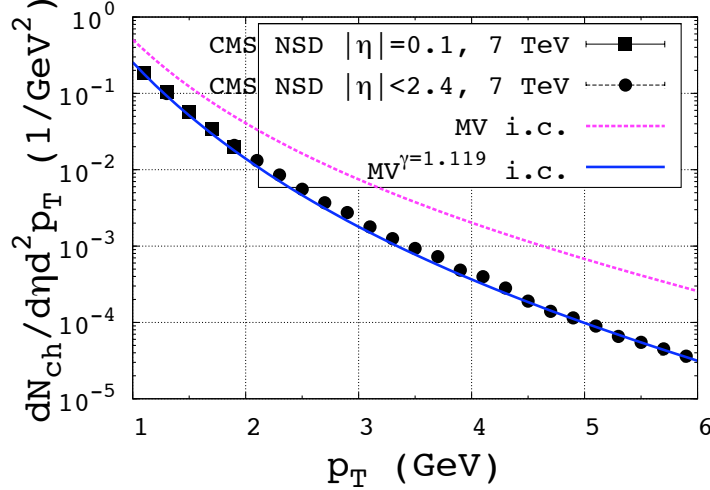


Figure 4: Transverse momentum distribution of charged particles at $\eta = 0$ for p+p collisions at $\sqrt{s} = 7$ TeV. CMS data from ref. [20].

For the range of p_{\perp} shown in the figure, particle production probes LC momentum fractions well below our assumed starting point of $x_0 = 0.01$. The uGD derived from MV model initial conditions is clearly too “hard” and predicts an incorrect slope. The new uGD obtained from the $MV^{\gamma=1.119}$ initial condition corrects this deficiency and provides a good description of the CMS data in the small- x , semi-hard regime (see, also, ref. [6]). This illustrates the power of LHC to constrain small- x physics. Also, we have used this observable to fix the genuine “K-factor” to $K = 2$ ($MV^{\gamma=1.119}$ i.c.) or $K = 1.5$ (MV i.c.), respectively.

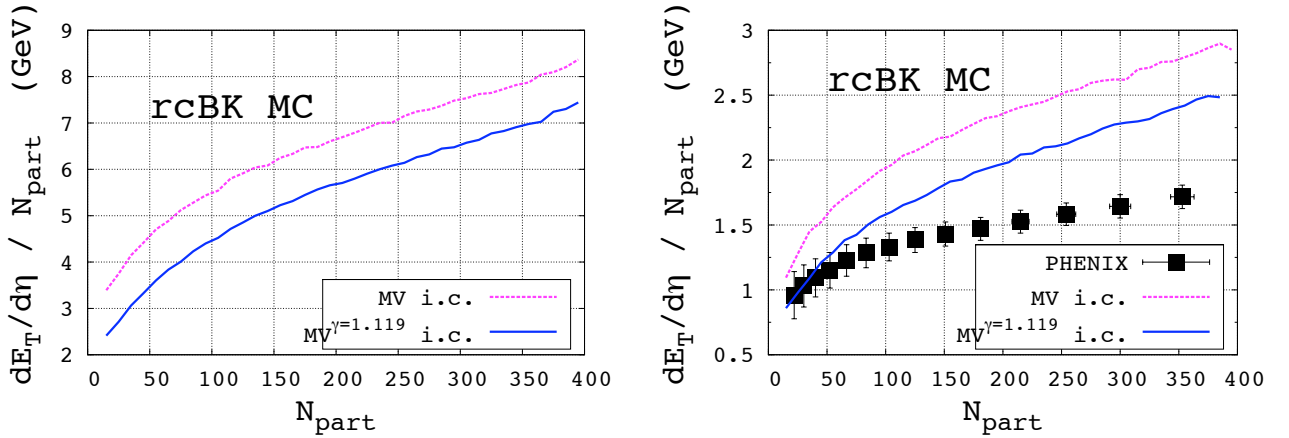


Figure 5: Transverse energy at $\eta = 0$ versus centrality for Pb+Pb collisions at $\sqrt{s} = 2.76$ TeV (left) and for Au+Au collisions at $\sqrt{s} = 200$ GeV (right).

The transverse energy in heavy-ion collisions versus centrality is shown in Fig. 5. The new $MV^{\gamma=1.119}$ uGD predicts a lower transverse energy than the one derived from MV model initial conditions, by about 1 GeV per participant at LHC energies⁴. It should be kept in mind that the measured transverse energy in the final state is only a lower bound on the initial $dE_{\perp}/d\eta$ since soft final-state interactions such as collective longitudinal flow do not conserve the transverse energy

⁴Note that we deviate from v1 of this manuscript in that the “gluon multiplication factor” κ_g has been dropped from the normalization for E_{\perp} .

per unit of rapidity [21].

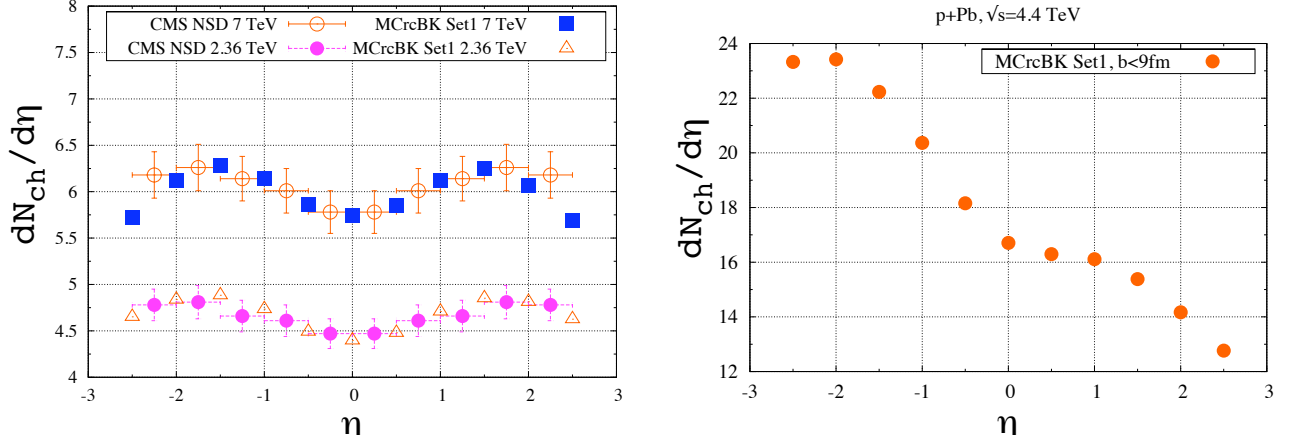


Figure 6: Charged particle pseudo-rapidity distributions for UGD Set 1 (MV model initial conditions) in pp collisions at 7 TeV (normalization adjustment -10%), 2.36 TeV (normalization adjustment -4%), and p+Pb collisions at 4.4 TeV (standard normalization as for AA collisions from Figs. 2, 3).

In Fig.6 we show the rapidity distributions in pp collisions at two LHC energies and a prediction for minimum bias p+Pb collisions at 4.4 TeV. We restrict these distributions to $|\eta| \leq 2.5$ since we have not accounted for the contribution of scattered valence partons. While there is perhaps an overall normalization uncertainty of up to $\sim 10\%$, we note the large forward-backward asymmetry for p+Pb collisions⁵ at rapidities far from the valence partons predicted by the rcBK-UGD.

We leave a more detailed study of the sensitivity of our results to the parameters of the model and a more detailed comparison with RHIC and LHC data for a future publication.

References

- [1] L. V. Gribov, E. M. Levin, and M. G. Ryskin, Phys. Rept. **100**, 1 (1983).
- [2] E. Iancu and R. Venugopalan, (2003), hep-ph/0303204.
- [3] H. Weigert, Prog. Part. Nucl. Phys. **55**, 461 (2005), hep-ph/0501087.
- [4] I. Balitsky, Nucl. Phys. **B463**, 99 (1996), hep-ph/9509348.
- [5] Y. V. Kovchegov, Phys. Rev. **D60**, 034008 (1999), hep-ph/9901281.
- [6] P. Tribedy and R. Venugopalan, Nucl. Phys. A **850**, 136 (2011).
- [7] Y. Kovchegov and H. Weigert, Nucl. Phys. **A 784**, 188 (2007), hep-ph/0609090.
- [8] I. Balitsky, Phys. Rev. **D75**, 014001 (2007), hep-ph/0609105.
- [9] E. Gardi, J. Kuokkanen, K. Rummukainen, and H. Weigert, Nucl. Phys. **A784**, 282 (2007), hep-ph/0609087.

⁵See also discussion of asymmetric collisions in ref. [22].

- [10] J. L. Albacete and Y. V. Kovchegov, Phys. Rev. **D75**, 125021 (2007), arXiv:0704.0612 [hep-ph].
- [11] J. L. Albacete, N. Armesto, J. G. Milhano, and C. A. Salgado, Phys. Rev. **D80**, 034031 (2009), 0902.1112.
- [12] J. L. Albacete, N. Armesto, J. G. Milhano, P. Quiroga Arias and C. A. Salgado, arXiv:1012.4408 [hep-ph].
- [13] J. L. Albacete, Phys. Rev. Lett. **99**, 262301 (2007), 0707.2545.
- [14] J. L. Albacete and C. Marquet, Phys. Lett. **B687**, 174 (2010), 1001.1378.
- [15] Y. V. Kovchegov and K. Tuchin, Phys. Rev. **D65**, 074026 (2002), hep-ph/0111362.
- [16] W. A. Horowitz and Y. V. Kovchegov, (2010), 1009.0545.
- [17] B. A. Kniehl, G. Kramer, B. Pötter, Nucl. Phys. **B582**, 514 (2000).
- [18] PHOBOS, B. B. Back *et al.*, Phys. Rev. **C65**, 061901 (2002), nucl-ex/0201005.
- [19] K. Aamodt *et al.* [The ALICE Collaboration], Phys. Rev. Lett. **105** (2010) 252301; Phys. Rev. Lett. **106** (2011) 032301.
- [20] V. Khachatryan *et al.* [CMS Collaboration], Phys. Rev. Lett. **105**, 022002 (2010).
- [21] M. Gyulassy and T. Matsui, Phys. Rev. D **29**, 419 (1984); M. Gyulassy, Y. Pang and B. Zhang, Nucl. Phys. A **626**, 999 (1997); K. J. Eskola, K. Kajantie, P. V. Ruuskanen and K. Tuominen, Nucl. Phys. B **570**, 379 (2000); A. Dumitru and M. Gyulassy, Phys. Lett. B **494**, 215 (2000).
- [22] D. Kharzeev, E. Levin, M. Nardi, Nucl. Phys. **A730**, 448-459 (2004); Nucl. Phys. **A747**, 609-629 (2005).